Journal of Statistical Physics, Vol. 68, No. 1/2, 1992

Accuracy of Semiclassical Dynamics in the Presence of Chaos

Patrick W. O'Connor,[1] Steven Tomsovic,[1] and Eric J. Heller[1]

Received December 18, 1991

We review some of the issues facing semiclassical methods in classically chaotic systems, then demonstrate the long-time accuracy of semiclassical propagation of a nonstationary wave packet using the quantum baker's map of Balazs and Voros. We show why some of the standard arguments against the efficacy of semiclassical dynamics for long-time chaotic motion are incorrect.

KEY WORDS: Semiclassical dynamics; chaos; quantum maps.

1. INTRODUCTION

Semiclassical mechanics has suffered from some tenacious theoretical and practical problems ever since its debut in the form of the "old quantum theory." The key complication behind many of the most intriguing theoretical quandaries is the presence of chaotic dynamics. Until very recently, there has been good reason to be guardedly pessimistic in some ways about the eventual payoff of exploring the semiclassical mechanics of chaos. But now the field appears to be undergoing a renaissance. In the past few years, theories of eigenvalue spectra based on periodic orbits, such as curvature expansions[1] and Riemann–Siegel lookalike formulas,[2] have been producing some very encouraging results. Our work in the time domain has also been fruitful; results for the stadium billiard[3] and earlier results on the baker's map[4] have been producing some unexpected but pleasant surprises.

The study of the quantum mechanics of classically chaotic systems is known as quantum chaology. Most of the work in this field has taken place

[1] Departments of Physics and Chemistry, BG-10, University of Washington, Seattle, Washington 98195.

0022-4715/92/0700-0131$06.50/0

in the energy domain, a Fourier transform (by stationary phase) away from the time domain. Our own recent contributions have shown that semiclassical techniques can be perhaps more readily extended to chaotic dynamics by shifting the perspective from the *energy domain* to the *time domain*. In this way, considerable progress has been made in understanding not only the dynamics, but also (by explicit Fourier transform) the energy spectrum[6] and the stationary states[7] of chaotic Hamiltonians. We have found some remarkably accurate comparisons to exact quantum dynamics, even for chaotic systems.[3–5] In this contribution, we describe the general setting behind these emerging semiclassical techniques and present some new results concerning the time scale of the validity of the semiclassical approximation.

1.1. Chaos and Semiclassical Dynamics

The earliest form of semiclassical mechanics, the old quantum theory, was concerned only with integrable motion. In the work generally credited with being the first enunciation of the correspondence principle,[8] Bohr extended the old quantum theory to the calculation of the intensities of spectral lines, in addition to the spectral frequencies. He was able to do so only when the classical motion was regular. In 1917, Einstein remarked that nonintegrable motion exists and is not treated by the standard quantization schemes.[19]

In the years immediately following the discovery of quantum mechanics, little effort was expended in trying to understand the asymptotic $h \to 0$ properties of classically chaotic systems. In fact, the basic issues went largely unrecognized for the next 40 years. It was commonly thought that chaos was an issue to be faced only in the context of "large" many-body systems. The recent resurgence of interest in classical mechanics has brought to the fore systems with as few as two degrees of freedom characterized by an intricate intermixing of chaos and regular motion which continues down to an arbitrarily fine scale. It has become imperative to discover the quantum implications of such classically chaotic motion, since it is so ubiquitous.

1.1.1. Periodic Orbit Spectral Theories. Before the subject really became popular, Martin Gutzwiller gave a major impetus to quantum chaology with his pioneering work on developing a semiclassical theory of the energy spectrum which could in principle be applied equally well to both regular and chaotic motions. His efforts culminated in the Gutzwiller trace formula,[10] which relates oscillations in the quantum density of states to properties of the classical periodic orbits.

He began by examining the time-dependent Green's function

$$G(\mathbf{q}, \mathbf{q}'; t) = \langle \mathbf{q} | \exp(-i\hat{\mathscr{H}} t/\hbar) | \mathbf{q}' \rangle \tag{1.1}$$

As early as 1928, Van Vleck had described a short-time semiclassical approximation to this propagator which could be used with a generic Hamiltonian.[11] His formula took the form

$$G(\mathbf{q}, \mathbf{q}'; t) \simeq \left| \mathrm{Det} \left(\frac{\partial^2 S}{2\pi i\hbar \, \partial \mathbf{q} \, \partial \mathbf{q}'} \right) \right|^{1/2} \exp\left(\frac{iS}{\hbar} \right) \tag{1.2}$$

where the action $S(\mathbf{q}, \mathbf{q}'; t)$ is Hamilton's principal function. To calculate $S(\mathbf{q}, \mathbf{q}'; t)$, the classical trajectory needs to be found which leads from $\mathbf{q}'$ to $\mathbf{q}$ in time t. The action is then given by $S = \int dt \, \mathscr{L}$, the time integral of the Lagrangian $\mathscr{L}$ along the trajectory. This formula is directly applicable, however, only for the time regime where merely a single trajectory can be found meeting the specified boundary conditions. With chaotic dynamics, this regime is typically *extremely* short-lived. In extending this work to longer times by including the possibility of multiple classical paths,

$$G(\mathbf{q}, \mathbf{q}'; t) \simeq \sum_j \left| \mathrm{Det} \left(\frac{\partial^2 S_j}{2\pi i\hbar \, \partial \mathbf{q} \, \partial \mathbf{q}'} \right) \right|^{1/2} \exp\left[i \left(\frac{S_j}{\hbar} + \phi_j \right) \right] \tag{1.3}$$

Gutzwiller found it necessary to augment the actions for the various paths with phase shifts ϕ_j, and showed how the ϕ_j could be calculated.[6] These phase shifts arise from the trajectories passing through focal points, where, as with the classical turning points, the simplest semiclassical prescription breaks down due to a rapidly changing de Broglie wavelength.[12] We call the resulting Green's function the "Van Vleck–Gutzwiller propagator."

Once the semiclassical dynamics had been constructed, spectral information could be inferred with a time–energy Fourier transform. In particular, Gutzwiller studied the density of states $g(E)$,

$$\begin{aligned} g(E) &= \int dq \, G(\mathbf{q}, \mathbf{q}; E) \\ G(\mathbf{q}, \mathbf{q}'; E) &= \int \frac{dt}{2\pi\hbar} G(\mathbf{q}, \mathbf{q}'; t) \, e^{iEt/\hbar} \end{aligned} \tag{1.4}$$

The density of states is such that $g(E)\,dE$ gives the number of energy levels found between E and $E + dE$. The entire energy spectrum is represented by the exact density of states simply as $g(E) = \sum_i \delta(E - E_i)$, a sum of Dirac delta functions, one centered at each of the energy eigenvalues E_i. By invoking the semiclassical approximation to the propagator $G(\mathbf{q}, \mathbf{q}'; t)$ and

evaluating all integrals by the method of stationary phase, Gutzwiller developed a semiclassical formula for $g(E)$. Periodic orbits entered the theory as being the stationary phase "points" for the integrand; the resulting integrals depend only on properties of these orbits.

Gutzwiller's theory has seen many notable successes. For example, Berry and Tabor have since demonstrated that for regular dynamics, Gutzwiller's theory is equivalent to the WKB quantization rules.[13] The trace formula has also been successfully used to extract the lowest few energy levels of several strongly chaotic systems.[14] There are even several chaotic systems where periodic orbit spectral theories are known to be exact.[15]

This is not to imply that the trace formula is without problems. One notorious difficulty is that without some way to damp out the contributions from the longer period orbits, the sum over periodic orbits is, at best, conditionally convergent. Doubts have also been raised whether the trace formula is even capable in general of resolving individual energy levels very far above the ground state.[16] Despite these worries, though, Gutzwiller's work constituted a significant advance for the understanding of the asymptotic $h \to 0$ spectral properties of chaotic systems.

1.1.2. Scars in the Eigenstates. The investigations of the eigenstates have, for the most part, been concerned more with developing an adequate understanding of the states' *qualitative* and *statistical* properties than striving for a detailed description of individual states.[17-19] The early history of the field was dominated by the thought that the stationary quantum solutions would reflect, in good measure, the stationary classical solutions.[18] For classically ergodic motion, the expectation was that the eigenstates would be essentially featureless, random waves which, in some sense, uniformly accessed the classical energy shell.[19]

Out of this arose a simple model, proposed by Berry,[19] for describing the local statistical properties of the eigenstates. The requirement that the wavefunction had a well-defined energy was met by demanding that in the vicinity of a given point $\mathbf{q}_0$ the wavefunction was comprised of a superposition of plane waves

$$\Psi(\mathbf{q}) = \sum_j a_j \exp(i\mathbf{k}_j \cdot \mathbf{q} + i\varphi_j) \tag{1.5}$$

where the magnitude of every wavevector was fixed to the same value $k = |\mathbf{k}_j|$ determined by energy considerations, $h^2k^2/2m = E - V(\mathbf{q}_0)$. Aside from this restriction, though, the wavefunction was taken to be as random as possible. The phases φ_j, orientations of the wavevectors $\mathbf{k}_j$, and amplitudes a_j were all chosen randomly, and the sum was to be taken over

an effectively infinite number of such plane wave components. Stechel and Heller[20] built upon this by developing the idea of "quantum ergodicity" in which not only were the individual eigenstates "random waves," but the set of eigenstates were statistically independent of one another. Quantum ergodicity describes the highest degree of randomness possible in a conservative quantum system, and as such represents a baseline against which one can judge the actual behavior of a system.

It was later discovered, though, that such a degree of randomness is often incompatible with certain simple dynamical facts.[7] The original argument focused on the evolution of wavepackets $|\Phi(t)\rangle = \exp(-i\hat{\mathscr{H}}t/\hbar)\,|\Phi(0)\rangle$ which were initially well localized in both their coordinate and momentum extents. The central object of the discussion was the autocorrelation function $\langle\Phi(0)|\Phi(t)\rangle$ which, in a sense, monitors the amplitude that the evolving state $|\Phi(t)\rangle$ returns to the region of phase space from which it was launched. The spectral intensities $|\langle\Phi(0)|E_j\rangle|^2$, which measure how well the eigenstates access the phase space region occupied by the initial wave packet, can be calculated in terms of the autocorrelation function as

$$\begin{aligned} S(E) &= \int \frac{dt}{2\pi\hbar} \langle\Phi(0)|\Phi(t)\rangle\, e^{iEt/\hbar} \\ &= \sum_j |\langle\Phi(0)|E_j\rangle|^2\, \delta(E-E_j) \end{aligned} \tag{1.6}$$

If quantum ergodicity indeed provides an adequate model for describing the system, the evolution of a wave packet obtains a sort of simplicity. The center of the wave packet moves away from its original value with an initial velocity $\langle\hat{\mathbf{p}}\rangle/m$, causing the autocorrelation function to decay to zero. The packet rapidly spreads and subsequently begins a diffusive exploration of the energy shell. The diffusion is in fact so strong that the evolved wave packet never returns to the region of the initial state as a coherent entity. The behavior of the autocorrelation function, after the initial decay, is then governed by purely statistical considerations.

The quantum ergodic description is demonstrably incorrect for wave packets launched in the vicinity of short-period periodic orbits, even with strongly chaotic dynamics.[7] The wave packet returns to its origin spread along the unstable manifold by an amount depending on the Lyapunov exponent of the periodic orbit, generating a recurrence in the autocorrelation function that can rise well above the statistical expectations. From this, one is able to infer that the stationary states would be subjected to an enhanced probability density all along a certain set of qualifying periodic orbits due to a coherent interference, and with an approximate wave

packet dynamics one can calculate the magnitude of the enhancement. The qualifying orbits are those with classical frequency ω and Lyapunov exponent λ such that $\omega/\lambda \geqslant 1$. The resulting concentration of probability along certain periodic orbits were called "scars" of the periodic orbits, and the original work on the subject showed several prominent examples in the eigenstates of the stadium billiards.[7] Scars have since been studied in a variety of systems,[21] where they often occur with such a frequency that at least as many states appear scarred as not.

1.2. Time Scales

In many ways the *fundamental* semiclassical approximation is the Van Vleck–Gutzwiller time propagator, and the justification of the derivative theories (such as the energy-domain Green's function) lies in the fact that the semiclassical dynamics, up to a fixed time t, becomes increasingly more accurate as Planck's constant approaches a value of zero. The question of whether or not semiclassical theories are capable, in principle, of describing the spectrum and stationary states of chaotic systems ultimately rests on the determination of the time scale $\mathscr{T}_{SC}$ for which the semiclassical dynamics accurately reflects the quantum dynamics.

A crucial time scale that arises in this connection is the so called *break time* $\mathscr{T}_B$. The break time follows from uncertainty principle considerations, and is the minimum time required to be able to study features in the energy domain with a fine enough resolution to see individual energy levels. For a system with d degrees of freedom, the break time typically scales with Planck's constant as $\mathscr{T}_B \sim 1/h^{d-1}$.

Semiclassical spectral theories are faced with the difficulty that while the semiclassical dynamics does become more accurate for a *fixed* time t as $h \to 0$, it is not at all clear that the accuracy continues out to the h-dependent break time, which rapidly grows to infinity with decreasing h. This conundrum severely complicates the analysis of the semiclassical limit. Little is actually known about the time scale $\mathscr{T}_{SC}$ over which the semiclassical dynamics breaksdown, or thus whether it is even capable of describing the quantum dynamics over the entire time range $\mathscr{T}_B$. Consequently, it is still an open question whether the spectra and stationary states of chaotic systems are within the grasp of semiclassical theories in the very limit $h \to 0$ for which they are derived.

In the literature, opinions expressed on these issues have ranged widely. At one extreme lies the optimistic claim that the Gutzwiller trace formula provides an *exact* description of the quantum spectrum in the $h \to 0$ limit.[22] This hope has been bolstered, in part, by the aforementioned successes of the trace formula. If true, it would seem to require that

the semiclassical dynamics becomes ever more accurate throughout the entire pre-break-time regime and beyond as Planck's constant diminishes. At the other extreme lies the pessimistic estimation that the semiclassical dynamics remains accurate only over an *exceedingly* short time scale $t^* = \mathcal{O}(\ln(1/h))$ known as the *log time*.[23]

One way to envision the origin of a time logarithmic in $\hbar$ is to consider the autocorrelation function $\langle \phi(0) | \phi(t) \rangle$ for a wave packet initially centered on an unstable periodic orbit situated in a chaotic sea. For the shortest, least unstable orbits, the early-time behavior of the autocorrelation function is to fall rapidly from unity to near zero as the wave packet moves along the periodic orbit and remain small save at the multiple periods of the orbit when the dynamics bring the evolving state back into the region of phase space from which it was launched.[24] Due to the stretching of the wave packet along the unstable manifold, the strength of each subsequent recurrence is smaller by a factor of $\exp(-\lambda\tau/2)$ from the previous one, where λ is the positive Lyapunov exponent characterizing the orbit and τ is the period. Such motion can be understood by considering only the dynamics linearized about the periodic orbit. However, in a bounded system, the unstable manifold must at some point fold back upon itself and eventually lead to a further set of nonlinear recurrences. The onset of these "homoclinic" recurrences serves as a natural definition of the log time. The wave packet can be made to constrict onto the periodic orbit as $\hbar \to 0$ in a uniform manner by letting the widths of the wave packet scale as $\hbar^{1/2}$,

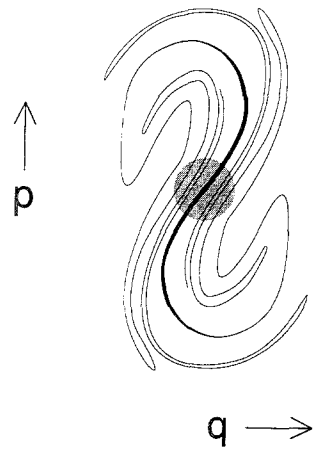

Fig. 1. A schematic representation of the homoclinic recurrences. The grey disk represents an initial swarm of trajectories whose evolved form is pictured in black; the propagation time just exceeds the log time. In this example, there are seven branches which contribute to the autocorrelation function. They proliferate exponentially.

causing the homoclinic recurrences to occur later and later. By coupling this with the exponential rate of spreading along the unstable manifold, one finds that the time scale for these recurrences does indeed scale as $\ln(\hbar^{-1})$.

Near this time, the homoclinic oscillations generate a proliferation of caustics.[25] Isolated caustics can easily be handled by uniformization techniques. However, by t^* or soon thereafter these corrections to the primitive semiclassical wavefunction become ubiquitous on the scale of a typical wavelength. Even if one were to uniformize the caustics, the log time would still be important because at this time the classical chaos is generating structural complexities (e.g., caustics) on the scale of a single quantum cell and smaller. The semiclassical dynamics generates an enormous number of contributions to $\langle \phi(0) | \phi(t) \rangle$ from the various branches of the homoclinic oscillations cutting through the initial state; see Fig. 1.

This evolving complexity can also be viewed from the standpoint of initial conditions. On the scale of a Planck cell, the different branches originate from imperceptible differences in initial conditions, thus contributing to the pessimism about the validity of semiclassical methods for such times in chaotic systems (however, see the Conclusion).

2. LONG-TIME DYNAMICS

The difficulties in quantum chaology have forced a temporary retreat to simplified systems. These include billiards on surfaces of constant negative curvature,[15] the Arnol'd cat map,[15] and a relative newcomer: the baker's map [26].[26] For our purpose of investigating the time scale question, the baker's map is an ideal starting point.

2.1. The Classical Baker's Transformation

The intricate structures and infinite complexities characteristic of chaotic Hamiltonians arise from an interplay of three essential ingredients. The first, Liouville's theorem, is one of the general principles of dynamics. The evolution may cause a region in phase space to become drastically distorted; however, Liouville's theorem guarantees that the volume encompassed by the region remains constant. The second is that the dynamics is locally unstable. Nearby trajectories separate exponentially fast, and a localized volume rapidly stretches into a thin, filamentary strand. The third is that the motion is bounded to a finite region in phase space, causing the filamentary volume to fold back upon itself, time and again, generating an ever more convoluted web.

The baker's transformation[27] is perhaps the simplest imaginable dynamical system that incorporates these three ingredients; it does so in a

very simple and visual manner. The phase space is restricted to a fundamental square $0 \leqslant q, p \leqslant 1$ which, as illustrated in Fig. 2, is mapped onto itself in a two-part transformation. The square is initially distorted into a rectangle with the q side stretched to twice its original length and the p side halved. The rectangle is then cut in half along the short axis and the two halves are stacked, the right on top of the left, to reform the fundamental domain. This transformation is codified with the mapping equations

$$\begin{aligned} q_{i+1} &= 2q_i - [2q_i] \\ p_{i+1} &= \frac{p_i + [2q_i]}{2} \end{aligned} \tag{2.1}$$

where the brackets are used to indicate the integer part of the argument.

2.1.1. Encoding the Dynamics. An attractive feature of this mapping is that the equations of motion can be exactly integrated and lead to a very simple relationship between the present and future positions of a trajectory. The integration is performed by a trivial construction which serves as a coding for the dynamics. Any given phase point (q, p) in the interior of the square can be fully specified by writing the coordinates as *binary* decimals, $q = .a_1 a_2 a_3 \ldots$ and $p = .b_1 b_2 b_3 \ldots$, and combining them back to back as $\ldots b_3 b_2 b_1 . a_1 a_2 a_3 \ldots$. The position of the decimal point separates q from p. The effect of each iteration of the mapping is merely to shift the

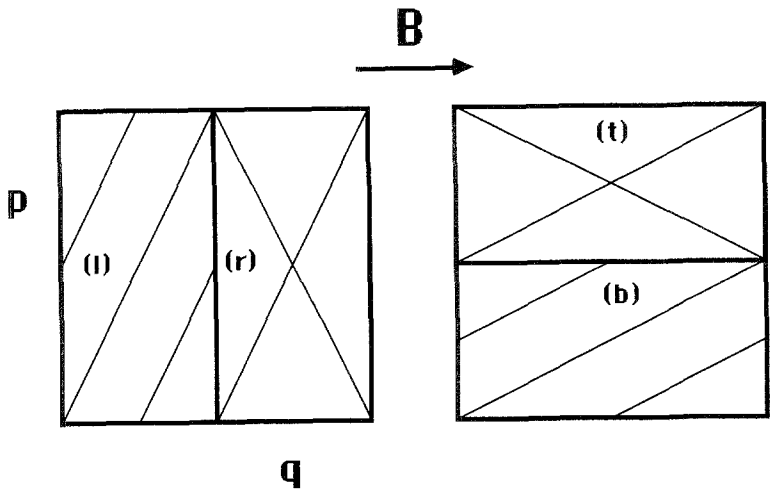

Fig. 2. Pictorial representation of one iteration of the classical baker's map, which is represented by the letter B. The left half, marked (l), is transformed into the bottom half (b) by a compression in p and stretching in q. Similarly, the right half (r) goes into the top (t).

decimal point to the right by one digit. The coordinate and momentum (q_t, p_t) of the trajectory after t mappings are then found by shifting the decimal point to the right by t digits. Reading to the right of the new decimal point gives q_t, whereas reading to the left gives the momentum p_t in a bit-reversed order. The entire history of the trajectory is thus laid out by the sequence of 0's and 1's in the coding $\ldots b_3 b_2 b_1 a_1 a_2 a_3 \ldots$, and the decimal point plays the role of discerning the present state.

Despite the simplicity of this transformation, the dynamics it generates displays the most highly chaotic motion possible in a Hamiltonian system. While the equations of motion are deterministic, any uncertainty in initial conditions is rapidly magnified to such an extent that after relatively few iterations of the map the trajectory can be found, with equal probability, anywhere in the entire phase space.

2.1.2. Correlation Functions. The encoding of the dynamics gives us a powerful descriptive tool. Consider the periodic orbits. Any point on a periodic orbit is a fixed point of the map iterated one full period. All of the fixed points of a given period t are easily located since their codings must have the special form $\ldots\gamma\gamma\gamma.\gamma\gamma\gamma\ldots$ of a subcode γ, containing t bits, which is repeated ad infinitum. A simple example of a period-three fixed point is $(1/7, 4/7)$. To identify the subcode of a period-t fixed point, one may start with the integer $\eta = (2^t - 1)\, q$. The subcode γ is just the binary representation of η with enough zeros added to the left to create a t-bit binary. Because the momentum is found from the coding by reading from right to left, rather than left to right, it is often convenient to define $\bar{\gamma}$ whose binary representation is found by reversing the ordering of the bits in the binary representation of γ. There is a similar relationship as above between γ and η, existing between $\bar{\gamma}$ and $(2^t - 1)\, p$ of the fixed point. The set of period-t fixed points is exhausted by allowing the integer η to vary over the range $0 \leqslant \eta \leqslant 2^t - 1$.

As illustrated in Fig. 3, the effect of iterating the baker's transformation t times can be given a simple, graphical interpretation. The phase space is thought of as being initially divided into 2^t identical vertical strips, each with a width $\delta q = 2^{-t}$. The γth strip spans the coordinate range $\gamma\delta q < q < (\gamma + 1)\, \delta q$. The choppings incurred by the t repetitions of the mapping all fall on the boundaries between strips. Each individual strip undergoes purely linear dynamics and after t iterations is transformed from a vertical to a horizontal strip which now stretches across the full breadth of the coordinate range and is compressed in momentum to a width $\delta p = 2^{-t}$. To complete the mapping, a rule is needed to specify how to stack these horizontal strips on top of one another to reform the phase space square. Clearly, if a period-t fixed point were to fall somewhere

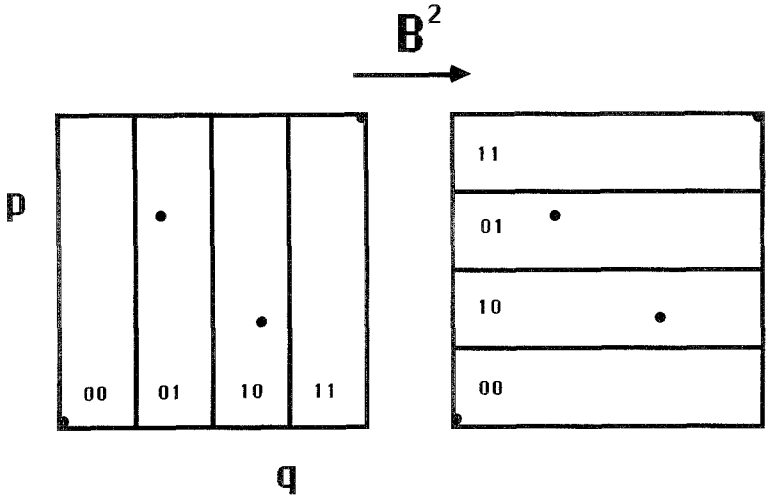

Fig. 3. Illustration of the organization by the fixed points of the twice-iterated map. The γ for each fixed point and strip is indicated.

within a given vertical strip, it would act as an anchoring point throughout the transformation, dictating exactly where the final horizontal strip is situated. The coding can be used to show that in every strip there must be one and only one fixed point, and the position of the fixed point in the γth strip is easily located because the subcode for the fixed point is the same integer as the strip label γ. As any particular strip can be interpreted as being the linearizable domain of the guiding fixed point, there arises the rather special situation that all the map's nonlinearities, which arise from the chopping, and, in fact, the evolution of the entire phase space can be completely incorporated by considering only the periodic orbits and the linear dynamics in their vicinity.

This organization leads to a very simple method for calculating the dynamical correlation function $\langle \rho_B \rho_A(t) \rangle$ between two phase space distributions ρ_A and ρ_B, where $\rho_A(t)$ is found by evolving the initial state ρ_A for t time steps. In this expression the brackets $\langle \cdots \rangle$ indicate an integration over the variables q, p. If the distribution ρ_B is taken to be highly localized to a particular region of phase space, the correlation function $\langle \rho_B \rho_A(t) \rangle$ serves to monitor the amount of the state ρ_A which is to be found in that region at time t. The method for calculating $\langle \rho_B \rho_A(t) \rangle$ is illustrated in Fig. 4 for an autocorrelation function $\rho_B = \rho_A(0)$, where the initial state is taken to be Gaussian-distributed in both coordinate and momentum. When considering the dynamics for a sufficiently long time t, the initial distribution ρ_A will generally be found to be spread over several

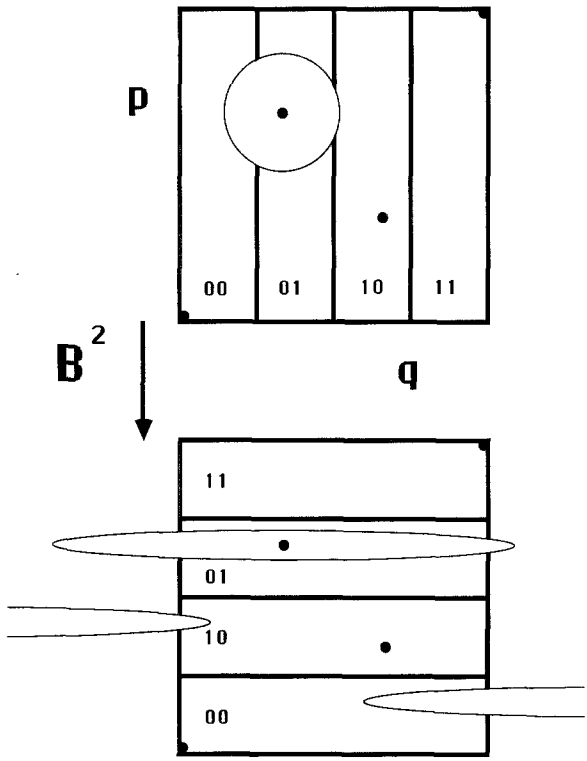

Fig. 4. In calculating the classical correlation functions, the initial distribution, pictured at top, is separately evolved by the linear dynamics of each strip into the distributions shown in the lower picture.

adjacent vertical strips. We will denote the contribution to $\langle \rho_B \rho_A(t) \rangle$ from that part of ρ_A which lies in the γth strip as $\langle \rho_B \rho_A(t) \rangle_\gamma$, and thus the entire correlation function will be given as

$$\langle \rho_B \rho_A(t) \rangle = \sum_\gamma \langle \rho_B \rho_A(t) \rangle_\gamma \tag{2.2}$$

A straightforward procedure for calculating $\langle \rho_B \rho_A(t) \rangle_\gamma$ would be to concentrate solely on that part of ρ_A which lies in the γth strip, apply the appropriate linear transformation to the strip, and then overlap the resulting distribution with ρ_B. An equivalent, but physically more appealing prescription is to evolve the *entire* state ρ_A by the linear dynamics of the γth fixed point, completely ignoring all choppings, and then overlap with ρ_B. From this point of view, the sum over γ is interpreted as being a sum over the fixed points. In this second method, every initial condition which

lies outside of the γth strip ends up outside of the fundamental phase space square. However, these unphysical trajectories are of no consequence to $\langle \rho_B \rho_A(t) \rangle_\gamma$, as the probe distribution ρ_B vanishes in these regimes.

2.2. The Quantum Baker's Map

In setting up the quantum description of the baler's transformation, we summarize the clear and intuitively appealing approach of Balazs and Voros.[26] It is convenient to work with a discretized coordinate space so that we need to specify the wavefunctions at only a finite number of lattice sites q_j rather than over a continuous range of positions q. The dimension of the Hilbert space needed to span the range of possible quantum states is thus kept finite, simply being equal to the number of lattice sites; we will work only with lattices with the even number of sites $2N$. From this restriction arises a natural definition of Planck's constant as $(2\pi\hbar)^{-1} = 2N$, since the $2N$ distinct quantum states are being supported, in a sense, by a classical phase space of unit area.

The momentum space is similarly discretized. Unless otherwise mentioned, the exact quantum results will be calculated using Saraceno's convention[28] for the placement of the lattice sites for the two representations:

$$q_j = \frac{1}{2N}\left(j + \frac{1}{2}\right) = p_j, \qquad j = 0,..., 2N-1 \tag{2.3}$$

Balazs and Voros originally used a slightly different convention. However, Saraceno showed that their lattice broke the R symmetry of the classical map, resulting in their quantum baker's map not respecting R. Using the lattice given by Eq. (2.3), Saraceno was able to restore the R symmetry to the quantized system. Transformation from the coordinate to the momentum representation is accomplished by a discrete Fourier transform denoted as G_{2N}; G_{2N}^{-1} then brings one back from p to q. The matrix elements of G_{2N} are the overlaps between eigenstates of p and those of q, and are given by

$$(G_{2N})_{jl} = \langle p_j | q_l \rangle = (2\pi\hbar)^{1/2} \exp(-ip_j q_l/\hbar) \tag{2.4}$$

While the lattice sites in Eq. (2.3) are restricted to lying within the fundamental domain, it is at times convenient to imagine the q (p) lattice as extending over the entire coordinate (momentum) axis. The wavefunctions are then thought to be periodically repeated, though the advancement of the coordinate or momentum by one unit is accompanied by a phase shift—i.e., $\psi(q+1) = \exp(i\phi_q)\psi(q)$ and $\psi(p+1) = \exp(i\phi_q)\psi(p)$.

Saraceno's convention results in $\phi_q = \pi = \phi_p$ antiperiodic boundary conditions for both the coordinate and momentum directions.

Rather than search for a generating function of the dynamics, Balazs and Voros chose to construct the evolution of a state by directly building a single time-step propagator $\hat{B}$ that was both the analogue of the classical evolution equations and manifestly unitary. They reasoned that the classical blockwise mappings $l \to b$ and $r \to t$ pictured in Fig. 2 could be captured in the quantum mechanics by specifying the state in a coordinate representation before the mapping, and in a momentum representation afterward. The $l \to b$ mapping was accomplished by Fourier analyzing the lower half $(q < 1/2)$ of the initial state to discern its momentum distribution. This information was squeezed into the lower half $(p < 1/2)$ of the final state, effectively halving all momenta. With similar considerations for the $r \to t$ mapping and a final Fourier transform to bring the entire state back into the coordinate representation, the full one-step propagator is given by

$$\hat{B} = G_{2N}^{-1} \begin{pmatrix} G_N & 0 \\ 0 & G_N \end{pmatrix} \tag{2.5}$$

For the rest of the work, we will drop the subscript denoting the dimension of the operators. Unless specified otherwise, all operators will act on the full, $2N$-dimensional vector space.

2.3. Nonlinear Wave Packet Dynamics

A fundamental goal of quantum mechanics is the means to predict transition amplitudes. For general dynamical systems, crudely stated, the semiclassical approximation to these amplitudes amounts to finding the classical routes for the transition, and associating the square root of a classical probability and a phase with each one. If there is anything general to be learned from the baker's map, it is necessary that a similar interpretation applies. The beautiful simplicity of the baker's map allows us to say, even before deriving it, what must be found. In order to incorporate the nonlinearities into the calculation of the quantum correlation function $\langle \phi_A | \hat{B}^t | \phi_B \rangle$, there must exist a semiclassical version of the classical method for obtaining $\langle \rho_A \rho_B(t) \rangle$ described near Eq. (2.2). The arguments which lead to an exact periodic orbit sum rule for the classical correlation functions also imply that the semiclassical calculation of correlation functions should take the form

$$\langle \phi_A | \hat{B}^t | \phi_B \rangle \approx \sum_{\gamma=0}^{2^t-1} \langle \phi_A | \hat{B}^t | \phi_B \rangle_\gamma \tag{2.6}$$

where the contribution from the γth fixed point, $\langle \phi_A | \hat{B}^t | \phi_B \rangle_\gamma$, is found by evolving the entire initial B state by the dynamics linearized about the γth fixed point, ignoring all cuttings, and then overlapping with the A state. This is the key to including the nonlinear effects of chopping into wave packet dynamics and, indeed, is precisely what falls out of a formal derivation of the long-time semiclassical dynamics; see the dissertation of O'Connor.[5]

For the sake of simplicity we will concentrate on the autocorrelation functions in the following. Localized wave packets of the form

$$\begin{aligned} \langle q | q_0, p_0, \sigma \rangle &= \sum_{j=-\infty}^{\infty} e^{ij\phi} g(q; q_0 - j, p_0, \sigma) \\ g(q; q_0, p_0, \sigma) &= \left(\frac{4\pi\hbar^2}{\sigma^2}\right)^{1/4} \exp\left(- \frac{(q-q_0)^2}{2\sigma^2} + \frac{ip_0(q-q_0)}{\hbar} \right) \end{aligned} \tag{2.7}$$

have as contributions from the γth fixed point

$$\begin{aligned} \langle q, p, \sigma | \hat{B}^t | q, p, \sigma \rangle_\gamma = \frac{e^{i\eta_\gamma}}{(\cosh t\lambda)^{1/2}} \exp\Bigg[&- \frac{\cosh t\lambda - 1}{2 \cosh t\lambda} \\ &\times \left(\frac{\delta q^2}{\sigma^2} + \frac{\delta p^2 \sigma^2}{\hbar^2} \right) - i \frac{\delta q \delta p}{\hbar} \tanh t\lambda \Bigg] \end{aligned} \tag{2.8}$$

where $\delta q = q - q_\gamma$ and $\delta p = p - p_\gamma$ are the distances of the center of the wave packet from the γth fixed point and $\eta_\gamma = (2^r - 1)\, p_\gamma q_\gamma / \hbar$. The result can be found by performing the appropriate Gaussian integrals and including the phases given in ref. 4. This specialization to the diagonal elements of the t-step propagator is done only for expository reasons. Indeed, the off-diagonal elements are crucial to the study of the manifestations of the nonlinear dynamics, both before and after t^*, in the stationary states.

2.3.1. Trace of the Propagator. Interest in the trace of the propagator, which we will denote as $\langle \hat{B}^t \rangle$, stems from the pivotal role it plays in the semiclassical understanding of spectral features. Knowledge of the propagator's traces for all times t is equivalent to a complete specification of the spectrum, since the time–energy Fourier transform of $\langle \hat{B}^t \rangle$ is the exact density of states. By evaluating $\langle \hat{B}^t \rangle$ with a semiclassical approximation to the dynamics, it is possible to associate features of the classical mechanics with their manifestations in the quantum spectrum.

For the calculation of $\langle \hat{B}^t \rangle$, we require a method of resolving the identity in terms of the wave packets. The similarity between the wave

packets defined on the discrete lattice and the more familiar continuous Gaussian coherent states suggests that this can be accomplished as

$$1 = \frac{1}{2\pi\hbar} \int_0^1 dp \int_0^1 dq \, |q, p, \sigma\rangle\langle q, p, \sigma| \tag{2.9}$$

which is easily shown to be true. The trace at time t is then calculated by evaluating the autocorrelation function $\langle q, p, \sigma | \hat{B}^t | q, p, \sigma \rangle$ as a function of the center (q, p) of the wave packet, and integrating over the centers. Invoking the above nonlinear semiclassical dynamics [Eq. (2.6) with $A = B$ and Eq. (2.8)] and interchanging the sum over fixed points with the integral over wave packets generates

$$\langle \hat{B}^t \rangle = \frac{1}{2 \sinh(\lambda t/2)} \sum_\gamma \exp(i\eta_\gamma) \tag{2.10}$$

The form taken by the semiclassical evaluation of $\langle \hat{B}^t \rangle$ nicely conforms with the usual expectations of periodic orbit theories.[29] The prefactor $[2 \sinh(\lambda t/2)]^{-1}$ is the appropriate weight for the various period-t fixed points, all of which are periodic without reflection and have the same stability properties.

2.4. Semiclassical Versus Quantum Correlation Functions

The quality of the semiclassical approximation may be illustrated by constructing a phase space map of the autocorrelation function magnitude, $W(q, p; t) = |\langle q, p, \sigma | \hat{B}^t | q, p, \sigma \rangle|$, for the entire ensemble of wave packets. By contouring the map $W(q, p; t)$ as a function of (q, p) for a succession of times t, one gains a more global view of the nature of the dynamics both before and after the log time. Saraceno[28] constructed the quantum version of this plot for $2\pi\hbar = 128^{-1}$. He found a sharp transition at the log time, before which there was an obvious quantum–classical correspondence and no interference phenomena present, but after which the opposite became true. He also called attention to an unusually strong set of recurrences in the vicinity of the period-two fixed points which peak at roughly twice the log time. These recurrences are so strong that the involved wave packets must be nearly completely reconstructed at a time when only statistical mixing is expected classically. Reproducing semiclassically such odd quantum behavior represents a severe test of the method since it is going to require a strong collective effect from the various terms in the autocorrelation sum if it is to work. We therefore recreate his plot and add alongside the semiclassical version. The maps for the times up to the log time are given in Fig. 5. The quantum and semiclassical figures are strikingly

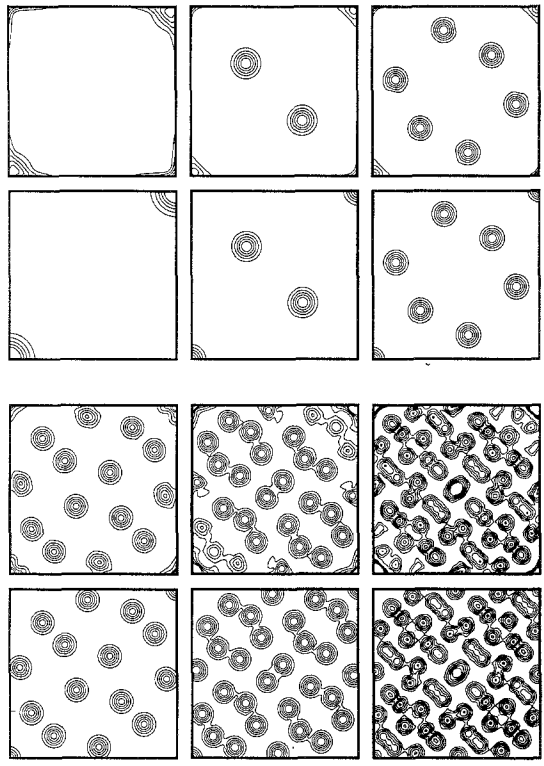

Fig. 5. Comparison of the quantum and semiclassical calculations of $W(q, p; t)$ for times $t = 1, 2, \ldots, 6$ (up to the log time). The p axis is vertical and the q horizontal. The five contours are equally spaced. The quantum version is shown immediately above the corresponding semiclassical figure. The local maxima are situated precisely on the classical fixed points.

similar, both looking essentially as the classical version would. The differences seen along the perimeter edges are to be expected for the reasons explained above. The invariance under reflection across either diagonal is simply due to the symmetries. The time progression continues in Fig. 6, starting from just beyond the log time and stretching to $2t^*$. The comparison of the quantum and semiclassical continues beautifully—the semiclassical dynamics is capturing nearly all of the interference patterns, including the late, large recurrences near the period-two fixed points. There is no longer any semblance of the purely classical dynamics remaining.

Surprisingly, in the baker's map the log time does not signal the breakdown of the semiclassical approximation. Could it be that this is a special feature of the baker's map? Two other systems, the Arnol'd cat map and tiling billiards on surfaces of constant negative curvature, are known

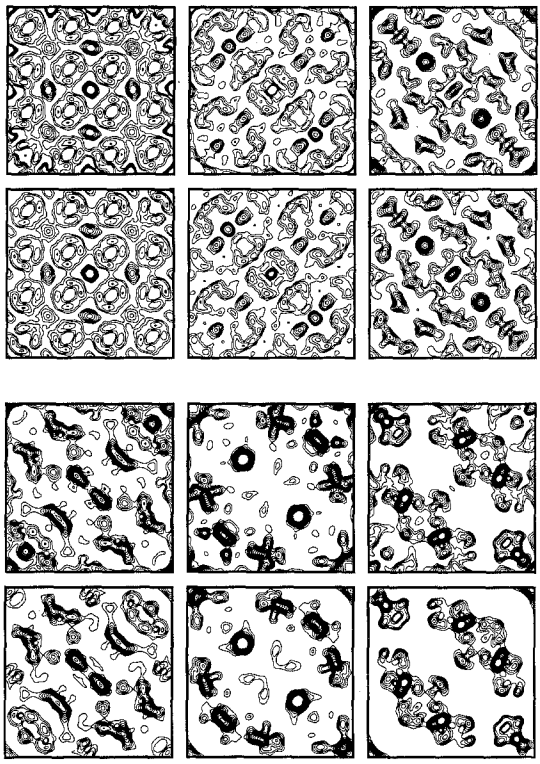

Fig. 6. Comparison of the quantum and semiclassical calculations of $W(q, p; t)$ for times $t = 7, 8, \ldots, 12$ (past the log time). The p axis is vertical and the q horizontal. The quantum version is shown immediately above the corresponding semiclassical figure. The contours are set at the same levels for all of the frames. Additional contours arise for the large peaks.

to lead to exact semiclassical formulas.[15] However, we have also seen excellent semiclassical dynamics in the post-log-time regime in a continuous dynamical system (as opposed to a discontinuous quantum map), the stadium billiard.[3] Billiards also have their peculiarities, but it may well turn out generally that the log time was far too pessimistic. If so, there remain fundamental questions of why the log time is not the breakdown time and what is the time scale on which semiclassical mechanics fails.

2.5. The Linear Time Scale

It is impractical, at least for the baker's map, to investigate the breakdown of semiclassical dynamics directly. Our direct attempts were blocked by the semiclassical approximation working as long in time as we

could practically calculate the summation over the classical orbits. The exponential proliferation of terms in the sum prevented us from continuing past $t \approx 4t^*$. A more feasible alternative approach is possible because an exact quantum meaning can be given to each individual γ contribution in the sums of Eqs. (2.6) and (2.10). Then an individual term may be studied quantum mechanically and semiclassically.

The quantum meaning of a γ decomposition is seen by constructing the path integral of $\hat{B}^t$ and organizing, in a natural way, groups of quantum paths corresponding to whether the paths sequentially find themselves on the left or right of the chopping line $q = 1/2$. There is not enough space to give the derivation here; it may be found in ref. 5 and some discussion is available from ref. 30. It becomes clear in deriving semiclassical dynamics from the path integral that, as would be intuitively expected, the most serious errors arise in the chopping zones, i.e., $q = 1/2$ and near the boundaries of the phase space square. An illustration of this feature can be constructed by finding the relative error in the semiclassical approximation $\langle \hat{B}^t \rangle_\gamma$. The collection of bad fixed-point contributions, i.e., those whose relative errors exceed 25%, show us where the semiclassical mechanics is breaking down. All the fixed points belonging to a particular periodic orbit have the same error, so it suffices to select just one fixed-point contribution per orbit. For a given orbit, selecting the fixed point which comes closest to the chopping zones gives Fig. 7 ($t = 14$; $2N = 128$). There is a narrow zone around the line $q = 1/2$ where the semiclassical approximation is failing. The effective width of this zone and its scaling properties with $\hbar$

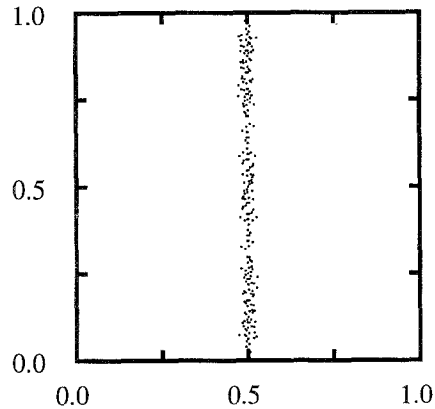

Fig. 7. Pictoral representation of the contributions to the trace of the propagator treated poorly by the semiclassical expression. The square represents the classical phase space. There is one dot per inaccurate periodic orbit contribution. It is drawn on that orbits' fixed point lying closest either to the square's boundary or the $q = 1/2$ line.

determine the time scale of the validity of semiclassical dynamics. A fairly sharp definition of the breakdown time τ_s can be given by adopting a criterion such as the time when, say, 1/4 of the periodic orbits have visited the chopping zone. Assuming that each periodic orbit only enters the zone of area (width) ω once at most, there are $\omega t 2^t$ bad fixed-point contributions out of a total of 2^t. The time τ_s approximately inversely proportional to the scaling with $\hbar$ of the width. In further tests, numerical evidence suggests the width decreases linearly with $\hbar$, which implies that $\tau_s \sim O(1/\hbar)$. This scale, though far longer than a log time, is on the boundary of being too weak to assure that the eigenstates and eigenvalues can be individually derived semiclassically.

3. DISCUSSION

Although the baker's map is a rather abstract system, we believe, following Balazs and Voros[26] and Saraceno,[28] that it contains not only the "essence of chaos," but also some rather generic quantum behavior. The influence of periodic orbits in the dynamics and in the eigenstates (in the form of scars) is well demonstrated in more physical systems and present, too, in the baker's map.

We have been able to go beyond earlier results on the baker's map, by showing that the semiclassical dynamics breaks down for most initial states on a time scale very long compared to the "log time" that had been expected. The reasons for this are not entirely clear, but at the same time it *is* clear that some of the old arguments for why semiclassical dynamics should not work past the log time were wrong. We list them below.

Fallacy 1. "Quantum mechanics smooths over structures in classical phase space which are smaller than $\hbar$." (This is true as far as it goes). "Therefore, such structures could not be used to construct a reasonable approximation to the quantum mechanics." This does not follow from the first, true statement, and is false! The time scale for such structures to appear globally is $\log(1/\hbar)$; this was the log time argument.

Fallacy 2. "Very close stationary phase points will give poor semiclassical results." This is definitely wrong as stated. The point here is that given the severe folding in chaotic dynamics, there are ways for stationary phase points (as viewed in some standard integral representation over position, or momentum, etc.) to become "close" while still not coalescing in the usual sense. As a fold in a formerly linear manifold first develops, suppose we mark off a loop that has area $\hbar$. Further dynamics will exponentially stretch the loop and bring the arms exponentially closer together, making the stationary phase points appear to be extremely close. However, this

proximity is an illusion, while the meandering loop still will have the same area in it. (The baker's map does not have loops in this sense, but has something even worse, i.e., the chopping of the classical manifolds).

Fallacy 3. "We can change the potential very slightly and drastically affect the long-time classical mechanics but not substantially affect the quantum mechanics." True, so far. "Therefore, the classical mechanics cannot possibly be used to construct an accurate semiclassical approximation." This is seen to be a variant of Fallacy 1.

Fallacy 4. "The Van Vleck Green's function generally has exponentially many caustics in it as time increases, and thus becomes useless." The first part of the statement is true, but the singularities are not fatal if we integrate over them (as in the propagation of a Gaussian coherent state). (The baker's map is an exception to this "problem," in that no loops with their attendant caustic tangencies are formed).

More work must be done to understand the breakdown of the semiclassical approximations, which this and our previous work have shown to be much more robust than previously thought.

One compelling (and sobering) fact is that as the classical mechanics gets more complex, it becomes increasingly difficult to calculate. As this and our previous studies have shown, it is possible to go well beyond the log time in the classical calculations, but probably not typically a factor of ten times the log time. We are working on ways to exploit the fact that the quantum mechanics is insensitive to some classical detail, in order to simplify the classical mechanics.

Applications to an increasingly wide array of physical problems are underway or contemplated. It is hoped that this will lead to new physical insight and permit calculations which were formerly too difficult.

ACKNOWLEDGMENTS

We wish to thank Miguel Sepúlveda for many stimulating discussions on the subject of chaos and quantum mechanics.

REFERENCES

1. P. Cvitanovic and B. Eckhardt, *Phys. Rev. Lett.* **63**:823 (1989).
2. M. V. Berry and J. P. Keating, *J. Phys. A* **23**:4839 (1990); E. B. Bogolmolny, *Commun. Atomic Mol. Phys.* **25**:67 (1990).
3. S. Tomsovic and E. J. Heller, *Phys. Rev. Lett.* **67**:664 (1991).
4. P. W. O'Connor and S. Tomsovic, *Ann. Phys.* (N.Y.) **207**:218 (1991); P. W. O'Connor, S. Tomsovic, and E. J. Heller, *Physica D* **55**:340 (1992).

5. P. W. O'Connor, Doctoral dissertation, University of Washington (1991).
6. M. C. Gutzwiller, *J. Math. Phys.* **10**:1004 (1969).
7. E. J. Heller, *Phys. Rev. Lett.* **53**:1515 (1984).
8. N. Bohr, On the quantum theory of line-spectra, in *Sources of Quantum Mechanics*, B. L. van der Waerden, ed. (North-Holland, Amsterdam, 1967).
9. A. Einstein, *Ver. Deut. Phys. Ges.* **19**:82 (1917) [English transl. by C. Jaffe, Joint Institute for Laboratory Astrophysics Report No. 116 (unpublished)].
10. M. C. Gutzwiller, *J. Math. Phys.* **12**:343 (1971), and references therein.
11. J. H. Van Vleck, *Proc. Natl. Acad. Sci. USA* **14**:178 (1928).
12. L. D. Landau and E. M. Lifshitz, *Quantum Mechanics* (Pergamon Press, New York, 1977).
13. M. V. Berry and M. Tabor, *Proc. Soc. Lond. A* **349**:101 (1976).
14. M. C. Gutzwiller, *Physica D* **5**:183 (1982); G. Tanner, P. Scherer, E. B. Bogomolny, B. Eckhardt, and D. Wintgen, *Phys. Rev. Lett.* **67** (1991).
15. N. L. Balazs and A. Voros, *Phys. Rep.* **143**(3):109 (1986); J. Keating, *Nonlinearity* **4**:309 (1991).
16. A. Voros, *J. Phys. A* **21**:685 (1988).
17. K. Uhlenbeck, *Am. J. Math.* **98**:1059 (1976); A. Voros, in *Stochastic Behavior in Classical and Quantum Hamiltonian Systems*, G. Casati and J. Ford, eds. (Springer-Verlag, New York, 1979); J. S. Hutchinson and R. E. Wyatt, *Chem. Phys. Lett.* **72**:378 (1980); M. V. Berry, in *Chaotic Behavior of Deterministic Systems*, G. Looss, R. Helleman, and R. Stora, eds. (North-Holland, New York, 1983); A. Peres, *Phys. Rev. A* **30**:504 (1984); M. Shapiro and G. Goelman, *Phys. Rev. Lett.* **53**:1714 (1984).
18. A. I. Schnirlman, *Usp. Mat. Nauk* **29**:181 (1974); S. Zelditch, *Duke Math. J.* **55**:919 (1987); Y. Colin de Verdiere, *Commun. Math. Phys.* **102**:497 (1985).
19. M. V. Berry, *J. Phys. A* **10**:2083 (1977).
20. E. B. Stechel and E. J. Heller, *Annu. Rev. Phys. Chem.* **35**:563 (1984).
21. D. Delande and J. C. Gay, *Phys. Rev. Lett.* **59**:1809 (1987); R. L. Waterland, J. Yuan, C. C. Martens, R. E. Gillilan, and W. P. Reinhardt, *Phys. Rev. Lett.* **61**:2733 (1988); E. J. Heller, P. W. O'Connor, and J. Gehlen, *Physica Scripta* **40**:354 (1989); B. Eckhardt, G. Hose, and E. Pollak, *Phys. Rev. A* **39**:3776 (1989); M. Saraceno, *Ann. Phys.* (N.Y.) **199**:37 (1990).
22. M. C. Gutzwiller, *Chaos in Classical and Quantum Mechanics* (Springer-Verlag, New York, 1990).
23. M. V. Berry and N. L. Balazs, *J. Phys. A* **12**:625 (1979).
24. E. J. Heller, in *Chaos and Quantum Physics*, M. J. Giannoni, A. Voros, and J. Zinn-Justin, eds. (Elsevier, Amsterdam, 1991).
25. M. V. Berry, N. L. Balazs, M. Tabor, and A. Voros, *Ann. Phys.* (N.Y.) **122**:26 (1979).
26. N. L. Balazs and A. Voros, *Europhys. Lett.* **4**:1089 (1987); *Ann. Phys.* (N.Y.) **190**:1 (1989).
27. V. I. Arnol'd and A. Avez, *Ergodic Problems of Classical Mechanics* (Benjamin, New York, 1968).
28. M. Saraceno, *Ann. Phys.* (N.Y.) **199**:37 (1990).
29. M. Tabor, *Physica D* **6**:195 (1983).
30. M. S. Saraceno and A. Voros, *Chaos* **2**:99 (1992).